AFRL-ML-WP-TP-2003-422

PROPERTIES OF CARBON NITRIDE FILMS DEPOSITED WITH AND WITHOUT ELECTRON CYCLOTRON RESONANCE PLASMA ASSISTANCE

Ming Y. Chen
Daniel J. Kramer

FEBRUARY 2001

Approved for public release; distribution is unlimited.

MATERIALS AND MANUFACTURING DIRECTORATE
AIR FORCE RESEARCH LABORATORY
AIR FORCE MATERIEL COMMAND
WRIGHT-PATTERSON AIR FORCE BASE, OH 45433-7750

REPORT DOCUMENTATION PAGE

1. REPORT DATE (DD-MM-YY)	2. REPORT TYPE	3. DATES COVERED (From - To)
February 2001	Journal Article	

4. TITLE AND SUBTITLE
PROPERTIES OF CARBON NITRIDE FILMS DEPOSITED WITH AND WITHOUT ELECTRON CYCLOTRON RESONANCE PLASMA ASSISTANCE

5a. CONTRACT NUMBER
IN-HOUSE

5b. GRANT NUMBER

5c. PROGRAM ELEMENT NUMBER
N/A

6. AUTHOR(S)
Ming Y. Chen
Daniel J. Kramer

5d. PROJECT NUMBER
N/A

5e. TASK NUMBER
N/A

5f. WORK UNIT NUMBER
N/A

7. PERFORMING ORGANIZATION NAME(S) AND ADDRESS(ES)
Nonstructural Materials Branch (AFRL/MLBT)
Non-Metallic Materials Division
Materials and Manufacturing Directorate
Air Force Research Laboratory, Air Force Materiel Command
Wright-Patterson AFB, OH 45433-7750

8. PERFORMING ORGANIZATION REPORT NUMBER
AFRL-ML-WP-TP-2003-422

9. SPONSORING/MONITORING AGENCY NAME(S) AND ADDRESS(ES)
Materials and Manufacturing Directorate
Air Force Research Laboratory
Air Force Materiel Command
Wright-Patterson AFB, OH 45433-7750

10. SPONSORING/MONITORING AGENCY ACRONYM(S)
AFRL/MLBT

11. SPONSORING/MONITORING AGENCY REPORT NUMBER(S)
AFRL-ML-WP-TP-2003-422

12. DISTRIBUTION/AVAILABILITY STATEMENT
Approved for public release; distribution is unlimited.

13. SUPPLEMENTARY NOTES
This material is declared a work of the U. S. Government and is not subject to protection in the United States.
Published in Thin Solid Films, Vol: 382, Issue: 1-2, pp. 4-12, February 1, 2001.

14. ABSTRACT
Research on carbon nitride has received considerable attention since β-C_3N_4 offers high technological potential for protective, wear, and optical applications. Deposition of carbon nitride by various techniques has mostly resulted in nitrogen deficient amorphous CN_x films. In this research, reactive magnetron sputtering with and without the assistance of an electron cyclotron resonance (ECR) source was used to deposit CN_x thin films at ambient temperature. The process variables include power level, nitrogen partial pressure, and substrate bias. X-ray photoelectron spectroscopy and Auger analysis were used to determine the composition and chemical bonding of the films. Ball-on-disc experiments were performed between 440C stainless steel balls and CN_x-coated 440C substrates at 0.1 m/s sliding velocity and 1 N load. The effects of process variables and interface modification on friction and wear rate were examined. Mechanical properties including hardness, modulus, and elastic response were obtained form nanoindentation. CN_x films with hardness in the range of 12-16 GPa demonstrated better wear performance than the hardest diamond-like carbon (24 GPa) deposited by the same technique. ECR assisted magnetron sputtering provided films with the lowest wear rates.

15. SUBJECT TERMS
Carbon nitride films; Electron cyclotron resonance plasma; Friction; Hardness

16. SECURITY CLASSIFICATION OF:			17. LIMITATION OF ABSTRACT:	18. NUMBER OF PAGES	19a. NAME OF RESPONSIBLE PERSON (Monitor)
a. REPORT Unclassified	b. ABSTRACT Unclassified	c. THIS PAGE Unclassified	SAR	16	Ming Y. Chen 19b. TELEPHONE NUMBER (Include Area Code) (937) 255-9099

Properties of carbon nitride films deposited with and without electron cyclotron resonance plasma assistance

Ming Y. Chen*, Daniel J. Kramer

Materials and Manufacturing Directorate, Air Force Research Laboratory, AFRL / MLBT, Wright-Patterson AFB, Dayton, OH 45433-7750, USA

Abstract

Research on carbon nitride has received considerable attention since β-C_3N_4 offers high technological potential for protective, wear, and optical applications. Deposition of carbon nitride by various techniques has mostly resulted in nitrogen deficient amorphous CN_x films. In this research, reactive magnetron sputtering with and without the assistance of an electron cyclotron resonance (ECR) source was used to deposit CN_x thin films at ambient temperature. The process variables include power level, nitrogen partial pressure, and substrate bias. X-Ray photoelectron spectroscopy and Auger analysis were used to determine the composition and chemical bonding of the films. Ball-on-disc experiments were performed between 440C stainless steel balls and CN_x-coated 440C substrates at 0.1 m/s sliding velocity and 1 N load. The effects of process variables and interface modification on friction and wear rate were examined. Mechanical properties including hardness, modulus, and elastic response were obtained from nanoindentation. CN_x films with hardness in the range of 12–16 GPa demonstrated better wear performance than the hardest diamond-like carbon (24 GPa) deposited by the same technique. ECR assisted magnetron sputtering provided films with the lowest wear rates. © 2001 Elsevier Science B.V. All rights reserved.

Keywords: Carbon nitride films; Electron cyclotron resonance plasma; Friction; Hardness

1. Introduction

Based on the theoretical calculations made by Liu and Cohen, β-C_3N_4 crystalline solid, which has the same structure as β-Si_3N_4, was predicted to have extreme hardness, comparable to or greater than that of diamond [1,2]. In addition to its predicted extreme hardness, carbon nitride may prove to be a novel material for device applications similar to β-Si_3N_4 and as a variable bandgap semiconductor [3]. Considerable effort has been directed toward the synthesis of this material by various deposition techniques including reactive dc and rf magnetron sputtering [4,5], ion beam

deposition [6,7], ion beam assisted deposition [8], chemical vapor deposition [9], pulsed laser deposition (PLD) [10–13], and ECR assisted electron beam evaporation of graphite [14]. Most carbon nitride (CN_x) films reported were amorphous and nitrogen deficient with $x < 1$. Evidence of nanocrystallites in a mostly amorphous carbon nitride film was reported [4,10–12]. However, the diffraction data obtained were not unique to the β-C_3N_4 structure that made unambiguous interpretation of the crystalline phase very difficult. Amorphous CN_x films are themselves useful since they have properties such as high hardness, variable optical band gap depending upon nitrogen content [15], and high chemical inertness. Currently, there is enormous interest in the replacement of amorphous carbon overcoats as wear resistant coatings in the magnetic thin film rigid disk recording industry. Carbon nitride films have high potential for this application.

---

*Corresponding author. Tel.: +1-937-255-9099; fax: +1-937-255-2176.

E-mail address: mingchen@wpafb.af.mil (M.Y. Chen).

We have grown CN_x films using dc magnetron sputtering as well as PLD. Our carbon nitride films were again all nitrogen-deficient with x ranging from 0.4 to 0.8 (30–45%) [16] and from 0.3 to 0.6 (25–40 at.% nitrogen) [13], respectively. PLD deposition at low pressure conditions (2 mtorr N_2) generated little or no nitrogen incorporation in the film. The utilization of a directed atomic nitrogen beam source was found necessary in order to achieve a higher nitrogen concentration. Similar results were reported by Niu et al. [12].

In this work, we focused on deposition of CN_x using dc magnetron sputtering with and without assistance from an electron cyclotron resonance (ECR) source for generating excited nitrogen species. ECR is an easy method to deliver a high density of low energy nitrogen species (tens instead of hundreds of electron volts for RF plasma) with enhanced ionization ratio. The motivation for this research was to explore the effect of additional low energy excited nitrogen species generated by an ECR source in enhancing nitrogen incorporation to achieve the β-C_3N_4 structure. The effects of process variables including target power level, nitrogen partial pressure and substrate bias, on the composition, chemical structure, morphology, and mechanical properties of CN_x films were studied.

2. Experimental

Films were deposited inside a stainless steel vacuum system equipped with an ASTEX (Applied Science and Technology, Woburn, MA) ECR microwave plasma source powered by a 100–700-W, 2.45-GHz power supply. The chamber was evacuated by a turbomolecular pump to a base pressure of 1×10^{-8} torr (1 torr = 133 Pa). A direct current (DC) magnetron sputtering source was used for film growth. A high purity graphite target was reactively sputtered. A schematic of the deposition apparatus is shown in Fig. 1. Ultra high purity nitrogen was used as the sputtering gas without any additional carrier gas. The process variables included total pressure (2–25 mtorr), target power (50–400 W), ECR power (100–400 W), substrate bias (ground, float, -50, -100, and -200 V), and substrate-to-target distance (d = 6–21 cm). The substrates used for CN_x coatings included 440C stainless steel disc (60 HRc, 25.4 mm diameter), 440C foil, and Si (100). Some ZnS substrates were also coated for future evaluation for potential rain/sand erosion resistant infrared (IR) applications. All substrates were ultrasonically cleaned in the sequence of acetone, methanol baths and then sputter etched in an Ar atmosphere just prior to each film deposition. The substrate was not intentionally heated except from exposure to the plasma during deposition which does not exceed 100°C. The nitrogen flow was normally held constant at 8 sccm. The deposition rates were determined from film thickness measurements
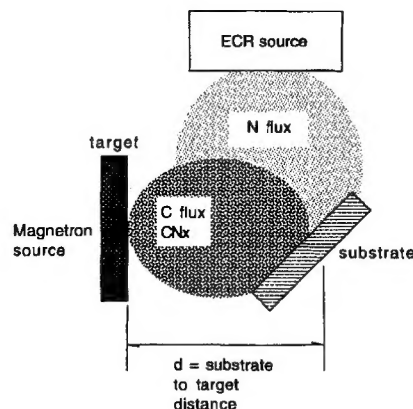

Fig. 1. Schematic diagram of the dc reactive magnetron sputtering system with electron resonance source mounted.

obtained from coated Si substrates using a surface profilometer (Dektak). Typical film thickness was in the range from 60 to 500 nm.

The microstructure and wear morphology were examined using scanning electron microscopy (SEM). X-Ray photoelectron spectra of films deposited with and without ECR assistance were obtained using a Surface Science Instruments M-Probe spectrometer. A monochromatic source of Al Kα X-ray was used to induce photoelectron emission. X-Ray photoelectron spectroscopy and Auger analysis were used to determine the composition and chemical bonding of the films. Tribological testing of the films was performed using a ball-on-disc tribometer. Some films were deposited on top of a Ti interlayer ($\sim$ 1500 A) for tribological evaluation of the benefit of a bonding layer. A Dektak profilometer was used to determine the width and depth of the wear tracks on the coated disks. Experiments were performed using 440C stainless steel balls and CN_x-coated 440C stainless steel discs at 0.1 m/s sliding velocity and 1 N load (Hertzian stress of 0.4 GPa). Mechanical properties including hardness, modulus and elastic response were measured using a NanoInstruments, Nanoindenter II with a Berkovich indentation head. Instrument calibrations were performed following the procedure developed by Oliver et al. [17].

3. Results and discussion

3.1. Film microstructure and chemistry

SEM micrographs for a typical CN_x film deposited with or without ECR assistance are shown respectively in Figs. 2b and 2a. It shows that the film microstructure was smooth, featureless and continuous (scratch marks remaining on substrate after polishing) except for deposition conditions involving low pressure (2 mtorr)
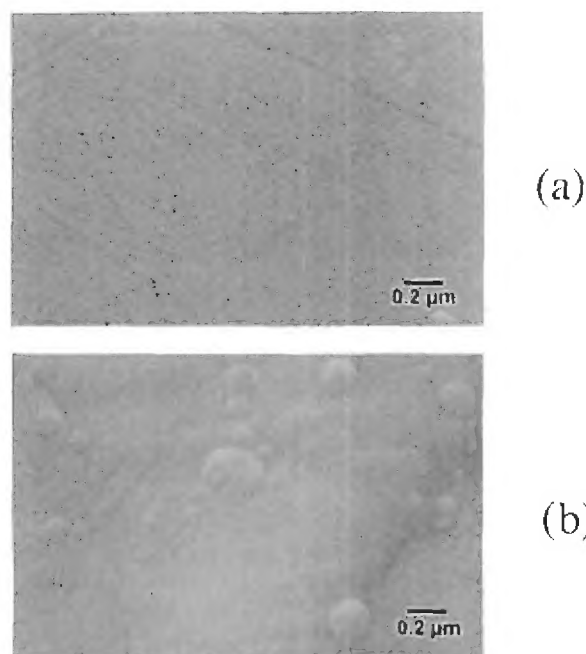
Fig. 2. Representative SEM micrograph of CN_x films deposited on 440C stainless steel: (a) with dc magnetron sputtering and (b) with ECR assisted dc magnetron sputtering.

and high ECR power (400 W). Under those conditions, some particles with sizes ranging from 0.06 to 0.25 μm were observed (Fig. 2b). As the ECR power decreases, there were fewer particles observed from SEM and the film surface was smoother.

Fig. 3 shows the deposition rates for CN_x films sputter deposited with and without ECR assistance and diamond-like carbon (DLC) films. All were deposited at 8 cm substrate to target distance. The DLC films were deposited using Ar instead of N_2 as the sputtering gas. The deposition rate is higher at lower pressure conditions. The deposition rate is approximately five times faster for CN_x films than for DLC films. This agrees with earlier reports showing the relation between N_2 pressure and sputter rate [4]. Using the ECR decreases the deposition rate of both DLC and CN_x. The
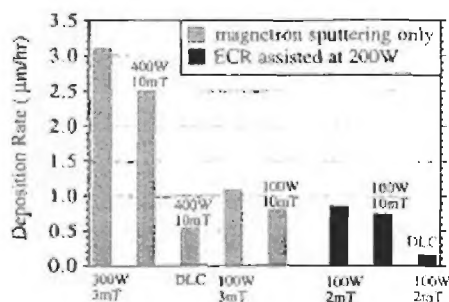

Fig. 3. Deposition rate for dc magnetron sputter deposited CN_x films and diamond-like carbon films with and without ECR assistance.
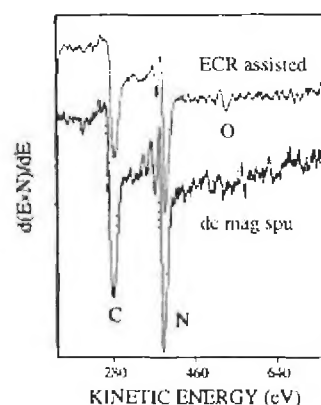

Fig. 4. Typical Auger spectra of CN_x films deposited with and without ECR assistance.

rate increases with increasing magnetron power and decreasing substrate-to-target distance. This is expected as the flux of depositing materials is enhanced with higher power and shorter substrate-to-target distance conditions.

Chemical information from the films was obtained from scanning Auger and X-ray photoelectron spectroscopy (XPS) analysis. Typical Auger spectra of films deposited with and without ECR assistance are shown in Fig. 4. The spectra were similar indicating that the films consist of mostly C and N. The carbon peak shape resembles that of DLC instead of graphitic C. The absence of substrate signals indicates that the film was smooth without large pinholes. Using the relative sensitivity factors given by Davis et al. [19], the highest nitrogen to carbon ratio, x, obtained in this study was 0.9 (48% atomic nitrogen). All the films deposited in
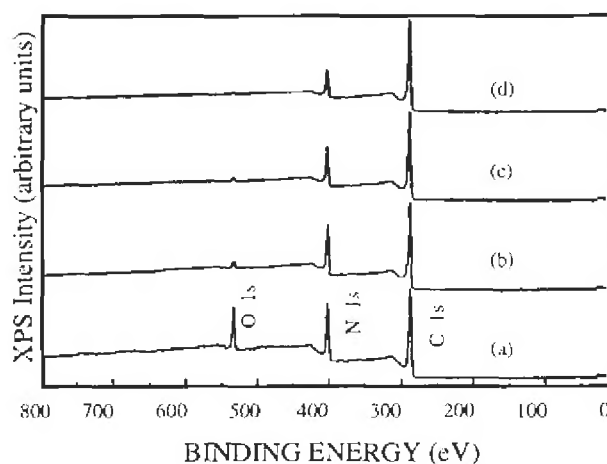

Fig. 5. XPS survey spectra from 0 to 1000 eV of a CN_x film: (a) as-deposited without any post-sputtering; (b) after 30 s; (c) after 1 min; and (d) after 2 min Ar sputtering. The film was deposited without ECR at 1500 W, 11 mtorr nitrogen, $d = 6$ cm, and substrate at floated condition.

this study were nitrogen deficient as compared to the predicted β-C_3N_4 with $x = 1.33$. Fig. 5 shows the XPS depth profile results of a CN_x film after 30 s, 1 min and 2 min Ar sputtering. This film was deposited at 1500 W, 11 mtorr nitrogen, and floating potential. The value of nitrogen content x drops from 0.36 for the as-received film to 0.34, 0.28, and 0.2 for the corresponding 30-s, 1- and 2-min sputtered film. The results show that the film suffered preferential sputtering of nitrogen. In addition to C and N, a small amount of oxygen (8–12%) was detected in the as-received films. With just 30 s light sputtering, the oxygen peak intensity decreases from 12 to 2.5%, indicating its presence is predominately near the surface region. The origin of this impurity is likely due to residual water vapor in the deposition chamber [20] and/or exposure to air during film transfer.

3.2. Effects of process variables

Negative substrate bias was found to decrease the nitrogen incorporation in the film. Even with a floating potential of ~ -15 V, the nitrogen positive ions with relatively low energy could still cause preferential removal of nitrogen similar to Ar sputtering. For a film deposited with ECR assistance, enhanced bombardment and re-sputtering by energetic species were also observed which explains the lower deposition rate. As the level of negative bias was increased to 100 V, no film accumulation was observed. Severe re-etching of the growing film prevented film growth.

Figs. 6 and 7 show the XPS N(1s) and C(1s) spectra of CN_x films deposited at 2 and 25 mtorr nitrogen pressure, 200 W ECR power and 100 W magnetron power. All the as-deposited CN_x films show similar nitrogen and carbon spectra. The N (1s) spectra were fitted with two peaks centered at 399.01 eV (N1) and 400.70 eV (N2). The peak at 399.01 eV is similar to the reported value for N≡C nitrile [21,22] that may form at the terminating end of a compound skeleton. The presence of N≡C peak is consistent with our IR and Raman result [4,16,18] with nitrile (C≡N) at 2200–2300 cm^{-1}. The N2 peak at 400.70 eV can be assigned to aromatic N=C bonds that may originate from N substituting C in an aromatic ring structure [23,24]. There were no distinct differences observed in N (1s) spectrum as a function of most process variables except a slight increase in the integral intensity of the 400.70-eV peak for the higher pressure condition (25 mtorr). The ratio of N1/N2 increased from 1.18 to 1.33 as the pressure is decreased from 25 to 2 mtorr. The effect of surface etching removal of aromatic N=C bonds as a result of ECR assistance is evidently more pronounced at low pressure than at high pressure. Preferential removal of aromatic N=C bonds may explain the observed higher N1/N2 ratio at 2 mtorr.
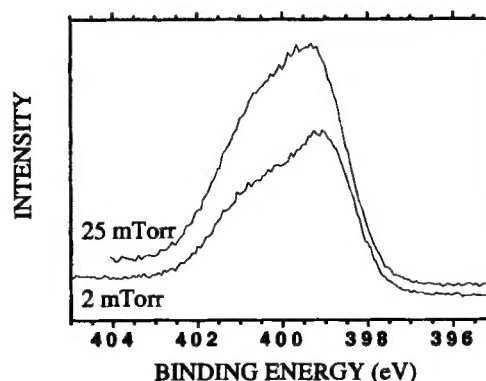

Fig. 6. Nitrogen (1s) spectra obtained from CN_x film deposited at 2 and 25 mtorr nitrogen, $d = 8$ cm, 200 W ECR power, 100 W magnetron power, and substrate at floated condition.

The carbon (1s) XPS spectra, shown in Fig. 7 can be fitted with three peaks at 288.67 eV (C1), 286.54 eV(C2) and 284.85 eV(C3). The XPS spectrum obtained from a diamond-like carbon (DLC) film deposited with pure argon at 10 mtorr without substrate bias at the same substrate-to-target distance is also included in this figure for comparison. The C(1s) peak positions for C3 and the DLC (284.66 eV) are similar to the reported value for amorphous carbon [25] (284.4–284.75 eV). C3 for CN_x can originate from amorphous carbon and adventitious surface carbon. The former is expected since the films were carbon-rich and a large fraction of the C atoms will thus have other C atoms as their nearest neighbors. The existence of carbon–nitrogen bonds would tend to transfer electron charge to the electronegative nitrogen instead of carbon, resulting in higher binding energies for the carbon core electrons. The higher binding energy values for C1 and C2 imply that their origins may be attributed to carbon bonded to nitrogen. Several researchers have attributed C2 to originate from the ring N=C bond [26–28]. The aro-
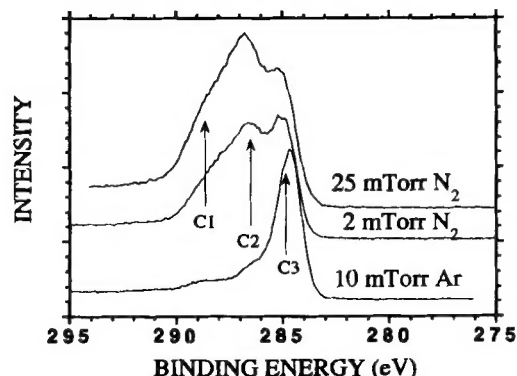

Fig. 7. Carbon (1s) spectra obtained from a DLC film deposited at 10 mtorr Ar, 400 W magnetron power, and CN_x film deposited at the same conditions as those shown in Fig. 6.

Table 1
Deposition parameters and the corresponding ratios of C1/C3, C2/C3, and N1/N2

Deposition conditions	Substrate to target distance (cm)	C1/C3	C2/C3	N1/N2	H (GPa)
3 mT, 150 W mag	16	1.34	0.73	0.99	–[a]
25 mT, 150 W mag	16	1.47	0.76	1.00	–[a]
3 mT, 1500 W mag	6	1.66	0.62	1.00	–[a]
11 mT, 1500 W mag	6	1.69	0.86	1.05	–[a]
2 mT, 100 W mag, 200 W ecr	8	0.65	2.7	1.33	15
25 mT, 100 W mag, 200 W ecr	8	1.23	0.87	1.18	1.5

[a] Hardness measurement could not be obtained due to either the film thickness was too thin or the substrate was not rigid (e.g. foil).

matic $N=C$ bonds are likely to arise from N substituting C in an aromatic ring structure. From our previous results [4,16,18], the predominantly IR inactive and Raman active sp^2 carbon absorption lines for DLC became IR active around 1546 and 1382 cm^{-1} for CN_x, indicating some nitrogen substitution in the aromatic ring structure. Parallel electron energy loss spectroscopy studies [18] also showed that carbon and nitrogen are predominantly sp^2-bonded to each other. Fujimoto and Ogata attributed C2 to be related to $C\equiv N$ triple bonding. However, ion bombardment of DLC film was also observed to contribute to more C2 instead of C3 intensity. The ratio of C1/C3 was found to decrease from 1.23 to 0.65 while C2/C3 ratio increase from 0.87 to 2.7 as the deposition pressure decreased from 25 to 2 mtorr. The nitrogen content in the film decreased as the pressure is decreased giving rise to a higher C3 intensity. Higher degree of ion bombardment at low pressure is likely to decrease C3 and increase C2 contribution. According to Rossi et al. [20], C1 can be associated with $C=N_2$ bonds. It can also assigned to CO bonds which formed at the surface of the films upon air exposure, prior to XPS analysis [28]. Fujimoto and Ogata [8] attributed C2 to be related to CN triple bonding. From our previous results [4,16,18], the predominantly IR inactive and Raman active sp^2 carbon absorption lines for DLC became IR active around 1546 and 1382 cm^{-1} for CN_x, indicating some nitrogen substitution in the aromatic ring structure.

Fig. 8 shows the C(1s) spectrum for CN_x films deposited without ECR assistance at the same conditions. The N (1s) spectrum showed similar results as a function of most process variables whether the film was deposited with or without ECR assistance. The deposition conditions of samples, substrate-to-target distance (d) and corresponding ratios of C1/C3, C2/C3, and N1/N2 are tabulated in Table 1. The ratio of N1/N2 remains relatively constant for a given deposition condition except when the film was deposited with ECR assistance at low pressure. Comparison of the overall C (1s) spectra for films deposited with and without ECR assistance showed that the integral intensity of the C1 peak is the highest for films deposited without ECR

assistance at high pressure or high substrate to target distance. In addition, the ratio C1/C3 becomes higher as the pressure is increased. This indicates that formation of $C=N_2$ or CO adsorption is favored at higher pressure. The C2/C3 ratio increases slightly for films deposited without ECR assistance while the ratio decreases for films deposited with ECR assistance as the deposition pressure is increased. The C2 peak is also observed to be the dominant peak for ECR assisted films at low pressures (2–10 mtorr).

The effects of process variables on the film composition were also explored. In general, the nitrogen to carbon ratio, x, for magnetron sputter deposited films with ($x = 0.3$–0.6) and without ($x = 0.4$–0.9) ECR assistance tends to decrease with increasing magnetron power or decreasing substrate to target distance. Higher ratios were achieved at high nitrogen pressure (25 mtorr instead of 2 mtorr). At low target power (100 W), the nitrogen to carbon ratio was 0.8, indicating resputtering due to energetic species is less. For magnetron powers of 500, 1000 and 1500 W, the nitrogen to carbon ratios were similar ($x = 0.4$ at 6 cm substrate-to-target distance) and independent of substrate bias
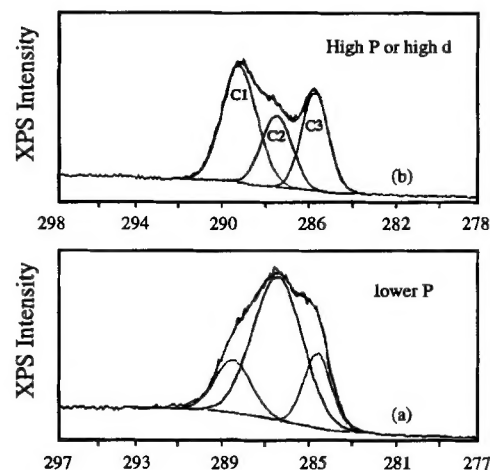

Fig. 8. Carbon (1s) spectra obtained from CN_x film deposited without ECR assistance at $d = 8$ cm: (a) 10 mtorr, 100 W magnetron power; and (b) 25 mtorr, 150 W magnetron power.

and total pressure (3–11 mtorr). For a given C/N ratio arriving at the growing film surface, the nitrogen to carbon ratio in the film can be attributed to the flux and the energy levels of the depositing species which in turn, are influenced by the deposition conditions. High deposition pressure and large substrate-to-target distance conditions would generate lower flux in reaching the substrate surface. The depositing species would have lower energy due to gas scattering, thus causing less preferential removal of nitrogen and x is higher. Recombination of atomic nitrogen is also more likely to occur at these conditions. On the other hand, conditions with high power, high pressure, or small substrate-to-target distance would produce high level of flux, resulting in the observed low, x, value.

3.3. Hardness and tribological properties

The carbon XPS spectra for films deposited at various conditions including pressure, power level, with or without ECR assistance, and substrate-to-target distance were similar to that shown in Fig. 8a,b. The respective peak width (full width half maximum) of C2 were found to be in two ranges: 1.16–1.60 eV and 2.22–3.05 eV. The C2 peak broadening was observed for films deposited at conditions with low pressure, high magnetron power or high ECR power. These deposition conditions favor enhanced ion bombardment during deposition. This peak broadening was similarly observed with C2 = 1.60 eV with floating condition and 2.59 eV for −50 V substrate bias conditions when deposited at 10 mtorr and 100 W target power. The latter would have a higher degree of ion bombardment contributing to the peak broadening observed. The corresponding ratios of carbon integral intensity obtained from XPS, C1/C3 and C2/C3, as a function of film average hardness are shown respectively in Figs. 9 and 10 for films with narrow and broad C2 peak. From Fig. 9, the hardness was found to be a low value whenever the intensity of C1 is high and C2 peak width is small. The hardness also tends to increase with increasing relative intensity of C3 (corresponding to C–C bond) as suggested by the decreasing ratio of both C1/C3 and C2/C3 when C2 peak width is small (Fig. 9). When the C2 peak width is broad (Fig. 10), the hardness seems not be correlated with the C1/C3 value: the hardness ranges from 2 to 15 GPa for C1/C3 = 0.6–0.8 and the higher hardness (15 GPa) is obtained for the highest C2/C3 value (2.7). The DLC films grown using the same deposition technique have the highest C3 intensity and film hardness (24 GPa) among all the films deposited in this study. Fig. 11 shows the average hardness of CN_x films deposited without and with ECR (200 W) assistance at the deposition conditions of 100 W magnetron target power and
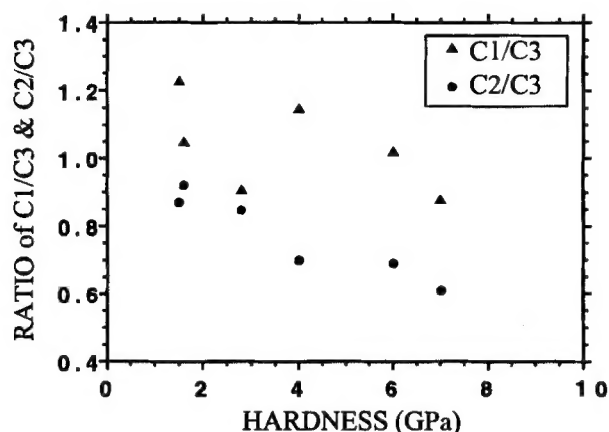

Fig. 9. Ratios of carbon (1s) integral intensity obtained from XPS, C1/C3 and C2/C3, as a function of film average hardness for films with C2 peak width = 1.16–1.60 eV.

8 cm substrate-to-target distance. There is a general trend of decreasing hardness with increasing deposition pressure. At a high deposition pressure or a large substrate-to-target distance, the integral intensity of C1 is high and the resulting films are always soft. Higher nitrogen pressure increases the probability of collision of the sputtered carbon with the nitrogen species, leading to bond formation between them forming the soft graphitic or $C=N_2$ material as opposed to hard C–N material.

At large substrate-to-target distance ($d > 14$ cm), the hardness of the films remained low regardless of the deposition pressure. However, we did not examine all the other deposition parameters for smaller substrate-to-target distance. At low nitrogen pressure, the range of hardness of the films was very large depending on the other deposition parameters. For films deposited
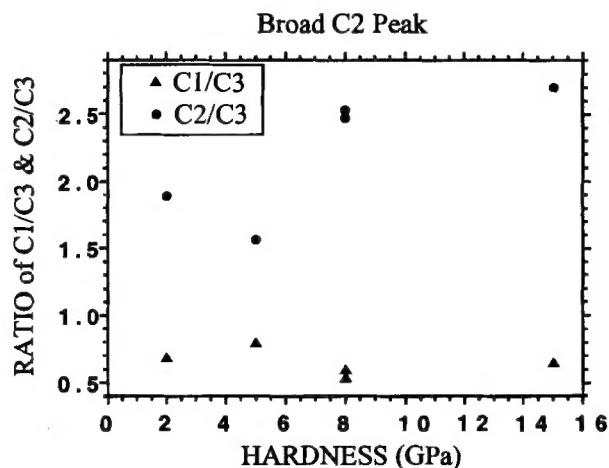

Fig. 10. Ratios of carbon (1s) integral intensity obtained from XPS, C1/C3 and C2/C3, as a function of film average hardness for films with C2 peak width = 2.22–3.05 eV.
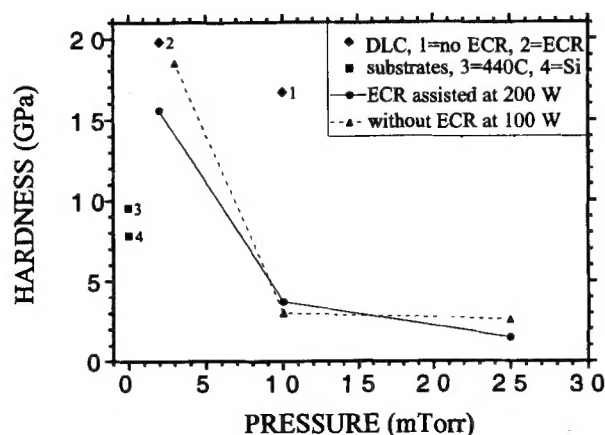
Fig. 11. Average hardness of CN_x films deposited without and with ECR (200 W) assistance. The films were deposited at 100 W target power and 8 cm substrate-to-target distance.

with Ar (DLC), the hardness was significantly higher than CN_x films that were deposited at 10 mtorr. At low deposition pressure (3 mtorr), the hardness of CN_x approached that of the DLC films.

The hardness as a function of magnetron target power and ECR assisted power level (x-axis) for films deposited without and with ECR assistance with 8 cm substrate-to-target distance is shown in Fig. 12. For the films grown at 3 mtorr without ECR assistance, there is an optimal power ($\sim$ 100 W) for obtaining the highest hardness. At this magnetron power level, ECR assisted deposition has resulted in lower hardness values for ECR power of 100–400 W. For a given 100-W target power, the ECR power at $\sim$ 200 W gives films with higher hardness.

The coefficient of friction (COF) was plotted against the total sliding distance in Fig. 13a,b for a typical CN_x film that was deposited with and without a Ti inter-
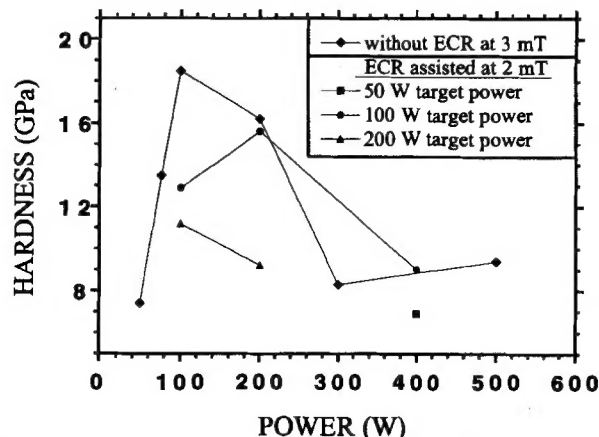

Fig. 12. Variation of average hardness as a function of power level (x-axis) of magnetron target power and ECR power for films deposited without and with ECR assistance, respectively.

layer, subjected to unlubricated ball-on-disc tribotesting in lab air with 40% relative humidity. The friction behavior of a DLC with a Ti interlayer was included in Fig. 13b for comparison. The COF for all CN_x films deposited in this study were found to be independent of the deposition conditions and were in the same range 0.20–0.25 with initial COF $\sim$ 0.16. Similar COF was obtained for DLC films grown with a Ti interlayer. The wear scars as examined by SEM are shown in Fig. 14. Films deposited without a Ti interlayer were adherent to the 440C substrate, however, they failed in a brittle mode under load at a shorter sliding distance than films deposited with a Ti interlayer. The films failed along the weakest interface instantly with the on-set of film fracture leaving large cracks running along the edge of the wear track. On the other hand, the occurrence of this sudden catastrophic damage to the film was not observed for films deposited with a Ti interlayer. Wear debris consisting of very fine particles along the two edges of the wear track was observed (Fig. 13b), instead of film delamination. From Fig. 13b, some spikes in the COF were observed when the CN_x film was tested beyond 1170 m sliding distance. The spikes indicated the generation of a few larger particles of wear debris arising from regions where some plowing and chipping away had occurred inside the wear track. Clearly, films deposited with a Ti interlayer showed much improvement in the film adhesion and wear life. The absence of these spikes for DLC suggests that the film adhesion for DLC was better than that of CN_x films to the Ti coated 440C substrates.

For films deposited with ECR assistance without a Ti interlayer, film delamination was observed in a few regions on the 440C and ZnS substrate surface after exposure to several days in an air environment. On the other hand, this was not observed for films deposited without ECR assistance, suggesting less compressive residual stress in the as-deposited films. Similar enhancement in the film adhesion and minimization of film delamination was achieved by adding a Ti interlayer.

From the friction tests, comparative wear rates (k) were calculated for the films by dividing the volume of removed material by the normal load and the sliding distance. The variation in wear rate with film hardness is shown in Fig. 15. The normalized volume wear rates were obtained from 1000-m sliding tests of CN_x and DLC films deposited with a Ti interlayer. Lower wear rates are generally observed for films with higher hardness. With the increased hardness from 1 to 16 GPa, the elastic recovery ranges from 40 to 79% and average effective modulus of 20–253 GPa were obtained. For CN_x films with hardness greater than $\sim$ 12 GPa, the wear rates were lower than that for the harder DLC film deposited. In addition, lower wear rates were observed for films deposited with than without ECR
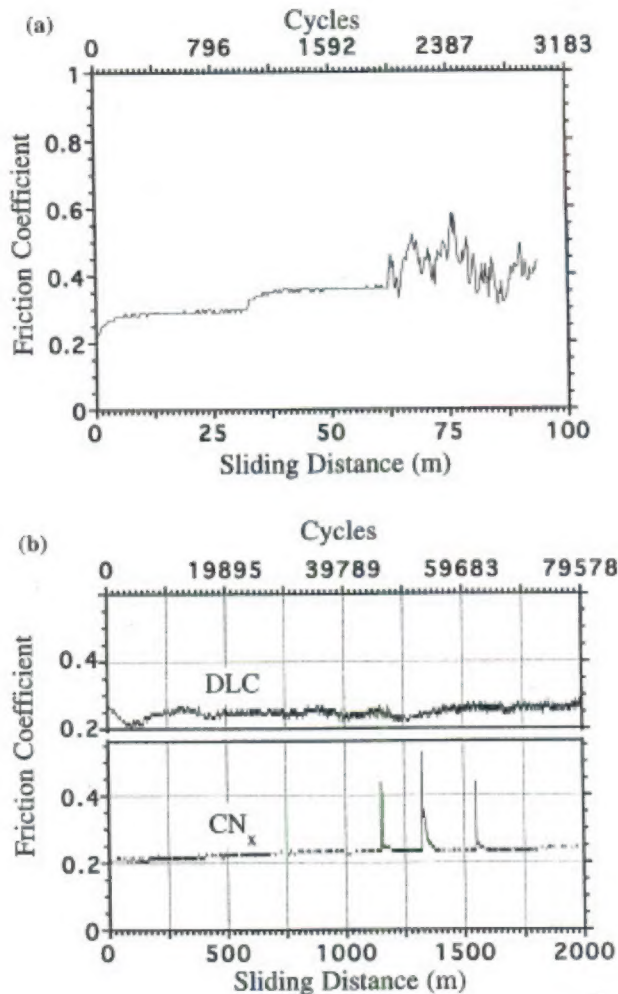
Fig. 13. Friction coefficient as a function of total sliding distance of: (a) a CN$_x$ film deposited without a Ti interlayer; and (b) CN$_x$ and DLC films deposited with a Ti interlayer.

Fig. 14. SEM micrograph of wear track surface obtained from the CN$_x$ film coated 440C disc after the unlubricated ball-on-disc test, shown in Fig. 13: (a) without a Ti interlayer; and (b) with a Ti interlayer.

assistance for these hard films. The wear rate of the best films grown using ECR assistance was found to be only half of that of DLC films deposited by the same technique when the film hardness was 15.6 and 23.8 GPa, respectively. This suggests that hard CN$_x$ film deposited by ECR assistance have great potential for tribological applications

4. Conclusion

Carbon nitride films were deposited using dc magnetron sputtering both with and without the assistance of an electron cyclotron resonance plasma source. The films were all nitrogen-deficient as compared to β-C$_3$N$_4$ with nitrogen content ranging from 0.3 to 0.9 (25–48 at.% nitrogen). The effects of process variables on film properties were examined. Higher nitrogen incorporation could be achieved by increasing the deposition
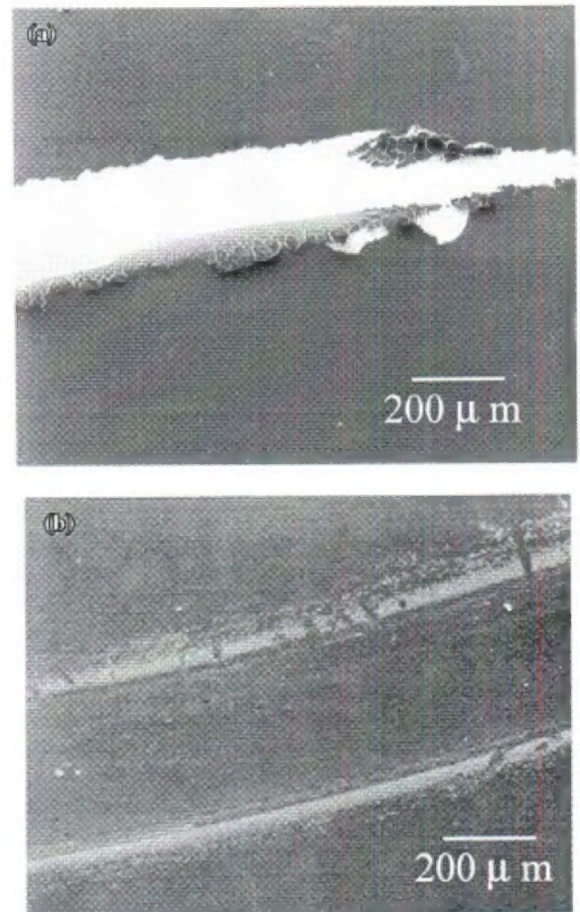
pressure and substrate-to-target distance without using ECR assistance. However, the chemical bonds favored at these conditions were weak bonds, consisting of
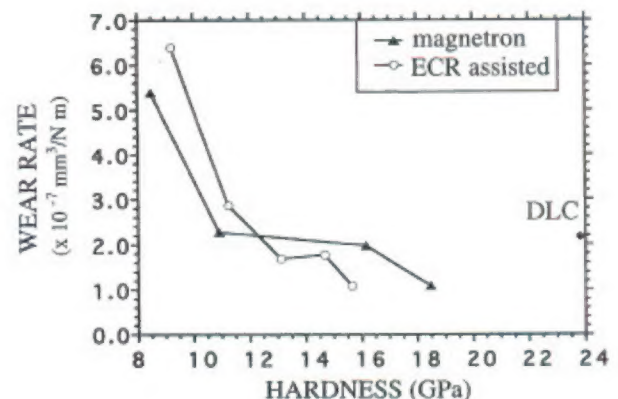

Fig. 15. Variation of wear rate with film hardness. Data were obtained from 1000-m sliding tests of CN$_x$ and DLC films that were deposited with a Ti interlayer.

$C=N_2$, aromatic $C=N$ bonds and $N\equiv C$ bonds instead of the strong β-C_3N_4 bonds. Negative substrate bias was found to enhance ion bombardment and sputtering which resulted in less film accumulation and lower nitrogen content. A wide range of hardness (1–16 GPa) was obtained by adjusting the deposition conditions. Low coefficients of friction (0.16–0.27) were obtained for unlubricated ball-on-disc testing against 440C stainless steel. Wear resistant CN_x films with hardness greater than ~ 12 GPa have shown wear rates lower than the hardest DLC films deposited by the same method. Lower wear rates were observed for these films deposited with ECR assistance. In this work, hard CN_x films deposited by dc magnetron sputtering with and without ECR assistance have demonstrated excellent wear resistance with high deposition rate (lower cost), indicating their good potential for tribological applications.

Acknowledgements

References

[1] A.Y. Liu, M.L. Cohen, Science 245 (1989) 841.
[2] A.Y. Liu, M.L. Cohen, Phys. Rev. B 41 (1990) 10727.
[3] S. Kumar, T.L. Tansley, Thin Solid Films 256 (1995) 44.
[4] M.Y. Chen, X. Lin, V.P. Dravid, Y.W. Chung, M.S. Wong, W.D. Sproul, Surf. Coat. Technol. 54/55 (1992) 360.
[5] T. Okada, S. Yamada, Y. Takeuchi, T. Wada, J. Appl. Phys. 78 (1995) 7416.
[6] D. Marton, K.J. Boyd, A.H. Al-Bayati, S.S. Todorov, J.W. Rabalais, Phys. Rev. Lett. 73 (1994) 118.
[7] S. Kobayashi, K. Miyazaki, S. Nozaki, H. Morisaki, J. Vac. Sci. Technol. A 14 (1996) 777.
[8] F. Fujimoto, K. Ogata, Jpn. J. Appl. Phys. 32 (1993) L420.
[9] J. Mort, M.A. Machonkin, K. Okumura, Appl. Phys. Lett. 59 (1991) 3148.
[10] Z.M. Ren, Y.C. Du, Y.X. Qiu, J.D. Wu, Z.F. Ying, X.X. Xiong, F.M. Li, Phys. Rev. B 51 (1995) 5274.
[11] C.M. Lieber, Z.J. Zhang, Adv. Mater. 6 (1994) 497.
[12] C. Niu, Y.Z. Lu, C.M. Lieber, Science 261 (1993) 334.
[13] M.Y. Chen, P.T. Murray, J. Vac. Sci. Technol. A16 (1998) 1.
[14] A. Bousetta, M. Lu, A. Bensaoula, A. Schultz, Appl. Phys. Lett. 65 (1994) 696.
[15] N. Voke, J. Kanicki, in: J.W. Coburn, R.A. Gottscho, D.W. Hess (Eds.), Plasma Processing, MRS, Pittsburg, 1986, p. 175.
[16] M.Y. Chen, Growth and Characterization of CN_x Films, Ph.D Thesis, Northwestern University 1994.
[17] W.C. Oliver, G.M. Pharr, J. Mater. Res. 7 (1992) 1564.
[18] M.Y. Chen, D. Li, X. Lin, V.P. Dravid, Y.W. Chung, M.S. Wong, W.D. Sproul, J. Vac. Sci. Technol. 11 (1993) 521.
[19] L.E. Davis, N.C. MacDonal, P.W. Palmberg, G.E. Riach, R.E. Weber, Physical Electronics Industries, Eden Prairie, MN, 1976.
[20] M. Andritschky, Vacuum 42 (1991) 753.
[21] B. Lindberg, A. Berndtsson, R. Nilsson, R. Nyholm, Acta Chem. Scand. A32 (1978) 353.
[22] B.S. Elman, M. Shayegan, M.S. Dresselhaus, H. Mazurek, G. Dresselhaus, Phys. Rev. B 25 (1982) 4142.
[23] B.J. Lindberg, J. Hedman, Chem. Sci. 7 (1975) 155.
[24] F. Rossi, B. Andre, A. Van Veen, P.E. Mijnarends, H. Schut, F. Labohm, M.P. Delplancke, H. Dunlop, E. Anger, Thin Solid Films 253 (1994) 85.
[25] J.C. Lascovich, R. Giorgi, S. Scaglione, Appl. Surf. Sci. 47 (1991) 17.
[26] M. Tabbal, P. Merel, S. Moisa, M. Chaker, A. Ricard, M. Moisan, Appl. Phys. Lett. 69 (1996) 1698.
[27] K.J. Boyd, D. Marton, S.S. Todorov, A.H. Al Bayati, J. Kulik, R.A. Zuhr, J.W. Rabalais, J. Vac. Sci. Technol. A13 (1995) 2110.
[28] P. Petrov, D.B. Dimitrov, D. Papadimitriou, G. Beshkov, V. Krastev, Ch. Georgiev, Appl. Surf. Sci. 151 (1999) 233.